**JURNAL SAINS MATERI INDONESIA (JUSAMI)**
ISSN: 1411-1098 (print), 2614-087X (online)
VOL. 26, ISSUE 2 2025
DOI: https://doi.org/10.55981/jsmi.5011

**ORIGINAL ARTICLE**

# The Effect of Ionic Liquid and Lithium Salt Electrolyte Addition on The Characteristics of Polyvinyl Alcohol/Chitosan-Based Membranes

R. S. Handika[1], C. R. Ratri[1,2], R. Rohib[3], and A. F. Nugraha[1, 4,*]

[1]Green Polymer Technology Laboratory, Department of Metallurgical and Materials Engineering, Faculty of Engineering, Universitas Indonesia, Depok, Indonesia
[2]Research Center for Advanced Materials, National Research and Innovation Agency of Indonesia (BRIN), South Tangerang, 15314, Indonesia
[3]Institut de Recherches sur la Catalyse et l'Environnement de Lyon, UMR 5256, CNRS 2 Avenue Albert Einstein, 69626
[4]Advanced Materials Research Center, Faculty of Engineering, Universitas Indonesia, Depok, 16424, Indonesia

**ABSTRACT** – The development of an environmentally friendly polymer electrolyte membrane for lithium-ion batteries is essential. A combined membrane composed of chitosan and polyvinyl alcohol (PVA) is one of the eco-friendly polymer membrane types used for lithium-ion battery electrolytes. The addition of ionic liquids and additives might improve the performance of the membrane. Therefore, this study examined the effect of ionic liquid 1-hexyl-3-methylimidazolium iodide (HMII) and lithium bis(oxalate) borate (LiBOB) electrolyte addition on the characteristics of composite membranes made of chitosan and PVA. Chitosan:PVA composition was made constant at 3:2, while the LiBOB was varied at 10, 25, and 40 wt.%. The HMII was added by 0.1 mL to ensure the HMII addition could be investigated. The results from scanning electron microscope (SEM), Fourier-transform infrared (FTIR), stress-strain test, and electrochemical impedance spectroscope (EIS) revealed that the addition of LiBOB and HMII was able to promote the agglomerations and the formation of microcrystals, which increased the mechanical properties and ionic conductivities of the membranes. The membrane sample with a LiBOB composition of 25% produced the highest mechanical properties with tensile strength of 21.11 MPa and elastic modulus of 1.93 MPa. The membrane sample with a LiBOB composition of 25% with the addition of HMII produced the highest ionic conductivity of 7.28 × 10-9 S/cm.

**ARTICLE HISTORY**
Received: 23 May 2024
Revised: 24 Jul 2024
Accepted: 17 Sep 2024

**KEYWORDS**
Chitosan,
Polyvinyl alcohol,
1-hexyl-3 methylimidazolium iodide ionic liquid,
Lithium bis(oxalate) borate electrolyte,
Li-ion battery

## INTRODUCTION

Lithium-ion (Li-ion) battery is one of the most promising secondary battery nowadays due to their wide useability for saving electric energy, both in communication and transportation [1],[2]. The electrolyte is considered one of the most important components of Li-ion batteries. Electrolyte facilitates lithium ions ($Li^+$) to transport freely between two electrodes so that the electric charge can be obtained, but electrolytes must be able to prevent short circuits between two electrodes [3]. In the application of electric transportation, which usually is a high-temperature system, an electrolyte that is stable in high-temperature conditions is required. Solid polymer electrolyte (SPE) has relatively better thermal, mechanical, and chemical stability than gel polymer electrolytes (GPE) and liquid electrolytes [4]–[6]. Recently, eco-friendly polymers, whether derived from natural substances or not, are highly desirable to support green energy campaigns [6].

One promising eco-friendly polymer is chitosan. As one of the natural polymers, chitosan can be obtained from living organisms like plant and animal body parts. From the exoskeletons of insects, shells of crustaceans, or various fungi, chitinous waste can be extracted biologically or chemically to produce chitin. In particular, the de-acetylation process of chitin will produce chitosan [7].

Chitosan is difficult to dissolve in water at neutral pH, so the ambient pH has to be lowered to facilitate the dissolution, such as by adding a weak acid. A very small concentration of weak acid is adequate to protonate the amine groups of chitosan to become a polar site so that chitosan can be dissolved in water [8]. Chitosan is a linear polysaccharide composed of randomly distributed de-acetylated units (β-(1,4)-D-glucosamine) and acetylated units (N-acetyl-D-glucosamine). Chitosan has amino groups and hydroxyl groups on its backbone, thereby giving it the polycationic characteristic. Due to this structure, chitosan has been studied for the development of electro-responsive materials [9].

However, the use of pure chitosan film is impractical due to its sensitivity to environmental conditions and poor mechanical properties. The flexibility of chitosan film can be improved by combining it with other polymers or a plasticizer [10]. There are many synthetic polymers mostly used in solid electrolytes, such as polystyrene,

***CORRESPONDING AUTHOR** | A. F. Nugraha | adam.febriyanto04@ui.ac.id

polyethylene oxide, polyvinyl alcohol (PVA), polycaprolactone, polymethyl methacrylate, polyvinyl chloride, polyvinyl pyrrolidone, and polyvinylidene fluoride. Among them, PVA is considered one of the most promising polymers due to several advantageous properties: relatively easy to fabricate, biodegradable, non-toxic, highly soluble in water, inexpensive, and odorless. PVA also exhibits high tensile strength, thermal stability, dielectric constant, and electrical capacity [11],[12]. Moreover, PVA has the hydroxyl (-OH) groups as the hydrogen bonding source, so a polymer complex can be constructed. The dissolution of salt in PVA is easier because of its polar group of hydroxy and its high chain flexibility [13].

Bernal et al. synthesized a nanofiber of PVA/chitosan using various compositions of chitosan. They found that the morphological uniformity of the membrane samples was poor if the composition of PVA was twice as much as chitosan. A ratio of chitosan:PVA of 4:5 produced better membrane uniformity. A lower concentration of chitosan diminished the entanglement and polymer–polymer interaction, thus causing chitosan to lose its fibrous structure and the morphological uniformity of the membrane [9]. Wardhono et al. did a similar study, but they added a crosslinking agent to increase the mechanical properties of the membrane [14].

As the chitosan content increased, the thermal stability of the chitosan/PVA membrane decreased, but the mechanical properties and the swelling degree of the membrane increased [9],[10]. Cheedarala and Song confirmed that combining chitosan with PVA increased the mechanical strength of the resulting membrane. The strain (%) and tensile modulus (MPa) of chitosan and PVA were 2.3 and 10.8 and 4 and 13.8, respectively. The chitosan/PVA membrane produced a strain (%) of 10.8 and tensile modulus (MPa) of 15.8 due to chemical cross-linking through the strong hydrogen bonding between chitosan and PVA [15]. Both chitosan and PVA have a hydroxyl group, which supports ionic exchange via the membrane, and chitosan has an amine group with a similar role. Combining chitosan with PVA will increase the membrane's ionic conductivity based on two possible reasons: a) the hydroxyl group of PVA increases the acidity of the membrane; b) the more the PVAs are added, the more the hydroxyl groups react with the amine groups of chitosan to form a polyelectrolyte complex [16].

PVA and chitosan show good compatibility with each other. Still, chitosan exhibits a major flaw: it reduces the crystallinity and strain capacity of the membrane, which increases the stiffness of the membrane [7]. To overcome this, the chitosan membrane can be treated with several lithium, ammonium, or sodium salts to improve its properties [8]. Previous studies have shown that the addition of Li, Ag, or Cu ions to the chitosan membrane was able to increase its ionic conductivity. The traditional lithium salts used in polymer electrolytes are $LiPF_4$, $LiClO_4$, $LiBF_4$, etc. [17]. Lithium bis(oxalate) borate (LiBOB) is a relatively biodegradable, cheap, and non-toxic lithium salt. It exhibits high thermal and electrochemical stability, high decomposition temperature (up to beyond 290°C), hygroscopic properties, low ionization in water, and is slightly soluble in propylene carbonates, esters, ketones, and lactones [18]. LiBOB has been used in previous studies to modify the properties of polymer-based membranes. For example, Khan et al. studied the effect of LiBOB addition to polymethyl methacrylate (PMMA) and polylactic acid (PLA) gel polymer blend (PMMA:PLA 80:20) [19]. LiBOB was found to alter the PMMA-PLA bond. LiBOB addition also affected the crystallinity of the sample, with 20 wt.% being the most amorphous. Yuan et al. added LiBOB to a Poly(vinylidene fluoride-co-hexafluoropropylene) (PVDF-HFP) membrane with additional lithium bis(trifluoromethanesulfonyl)imide (LiTFSI) as an ionic liquid. They observed the addition of LiBOB to increase the tensile strength and modulus. The addition of LiBOB also improved the ionic conductivity until a certain point where the ionic conductivity improvement was found to be insignificant [20].

Meanwhile, ionic liquids are liquids at room temperature that have low viscosity and melting point, are soluble in organic and inorganic solvents, and exhibit high electrical conductivity and good thermal stability [21]. The addition of ionic liquid will increase the ionic conductivity of the membrane [22]. Alkyl imidazolium, such as 1-hexyl-3-methylimidazolium iodide (HMII), is a commonly used ionic liquid for electrolyte application. HMII has an imidazolium group as a base structure, two alkyls with different chain lengths as side groups (6 carbon chain as hexyl and 1 carbon chain as methyl), and iodide ion ($I^-$). Therefore, it has an organic cation as the imidazolium group and an inorganic anion as iodide. HMII, as an ionic liquid, is a good candidate as a plasticizer for electrochemical applications because they have negligible vapor pressure, is non-flammable, thermally stable, chemically stable, and has high ionic conductivity [23]. Chew et al. used HMII to improve the ionic conductivity of gel polymer electrolytes made from polyacrylonitrile (PAN) [24]. Qin et al. found the optimum HMII addition amount to poly(1,6-hexanediol diacrylate) (PHDA) membrane to the function of its ionic conductivity. The miscibility of HMII to PHDA was suggested to affect the optimum HMII input to the membrane. Hence, different membrane constituents will lead to different membrane ionic conductivity properties [25].

Herein, we studied the effect of HMII and LiBOB addition on the characteristics of composite membranes made of chitosan and PVA. Our former sub-research already tried to make a combination of chitosan and PVA; the composition 9:1 for chitosan:PVA did not result in good membranes (too brittle), and 3:2 was better. Six membrane samples with a ratio of chitosan:PVA (3:2) and varied compositions of LiBOB electrolyte were prepared. The surface and chemical properties of the membranes were observed to determine how the addition of HMII and LiBOB affected the mechanical properties and ionic conductivity of the membranes.

## EXPERIMENTAL METHOD

### Materials and Instruments

All materials used in this study were purchased from Aldrich, including polyvinyl alcohol (PVA), ionic liquid 1-hexyl-3-methylimidazolium iodide (HMII), chitosan, and Lithium bis(oxalate) borate (LiBOB) electrolyte. All of these materials were obtained in pro analyst grade.

The equipment used in this paper was electrochemical impedance spectroscopy (EIS) Metrohm Autolab for electrochemical characterization, scanning electron microscope (SEM) Jeol-JSM IT-200 for morphological analysis, universal testing machine for mechanical characterization, and Fourier-transform infrared (FTIR) for functional group analysis.

### Method and Procedure

Firstly, PVA was diluted with deionized water, while chitosan was diluted with acetic acid of 1%. The PVA solution was then mixed with LiBOB salts of varied compositions and poured into the chitosan solution. Ionic liquid HMII was added to several solutions but not to several others. Each solution was then cast into the petri dish evenly and dried using silica gel for three days. The detailed composition of the samples used is displayed in Table 1.

**Table 1.** Composition of samples

| Sample code | Chitosan (% w/v) | PVA (% v/v) | HMII (mL) | LiBOB (% v/v) |
|---|---|---|---|---|
| KPL10 | 3 | 2 | - | 10 |
| KPL25 | 3 | 2 | - | 25 |
| KPL40 | 3 | 2 | - | 40 |
| KPIL10 | 3 | 2 | 0.1 | 10 |
| KPIL25 | 3 | 2 | 0.1 | 25 |
| KPIL40 | 3 | 2 | 0.1 | 40 |

The properties of the membranes produced were then characterized using scanning electron microscopy–energy dispersive X-ray (SEM-EDX), FTIR, a stress-strain test, and electrochemical impedance spectroscopy (EIS).

## RESULT AND DISCUSSION

### Surface and Cross-Section Appearance of Membrane Samples

Chitosan had to be dissolved first in acetic acid separately before mixing with the other materials. Acetic acid of 1% was used as a solvent for chitosan because chitosan is difficult to dissolve at neutral pH conditions. The amine groups of chitosan must first be protonated to become a polar site. This site plays a role in facilitating the solubility of chitosan in polar solvents, such as deionized water. In this stage, strong acids, such as hydrochloric acid or sulfuric acid, are not needed as they may oxidize the hydroxyl (-OH) groups of chitosan so that the final properties will be different. While weak acid can increase the polarity of chitosan, the degree of polymerization (DP) affects the solubility of chitosan in polar solvent. The higher the DP value, the longer the chitosan dissolves in polar solvents. While all materials used were mixed, ultrasonic treatment was important to decrease and control the bubbles that appeared. If the bubbles remain in the solution until the casting process, voids will be formed on the membranes' surface after the drying process.

As seen in Figure 1, almost all membranes produced low homogeneity in surface morphology. This may indicate that the LiBOB salt did not completely dissolve in the polymer matrix. This is possibly caused by LiBOB electrolytes triggering agglomerations and the formation of microcrystals during the drying process [8]. However, the phenomenon needs to be confirmed with a scanning electron microscope (SEM).

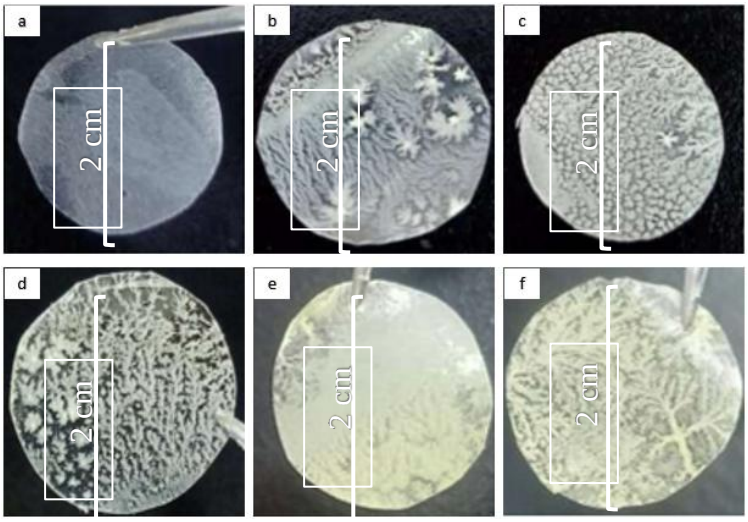


**Figure 1.** Surface morphology of the membranes produced: (a) KPL10, (b) KPL25, (c) KPL40, (d) KPIL10, (e) KPIL25, and (f) KPIL40

Figure 2 displays the SEM images of the membrane surfaces. Based on the results, the surface morphology of all samples looked dense. No clear pore was shown in all samples' surface and cross-section morphologies. Although the structures look rougher, there was no clear pore penetrating across membranes. Cross-section images of KPL samples were denser than the KPIL ones, confirming that the ionic liquid addition affected the structure of membranes to become rougher. In KPL and KPIL samples, the addition of LiBOB affected the structure of the membranes. The higher the LiBOB composition, the rougher the membrane structure morphology. Furthermore, rougher morphology indicated that there were nanopores, and a highly porous membrane produces higher electrolyte uptake as there are more microvoids for the electrolyte to pass through and be absorbed by the membrane. This higher electrolyte uptake facilitates better ionic transportation between membranes so that the ionic conductivity will increase.

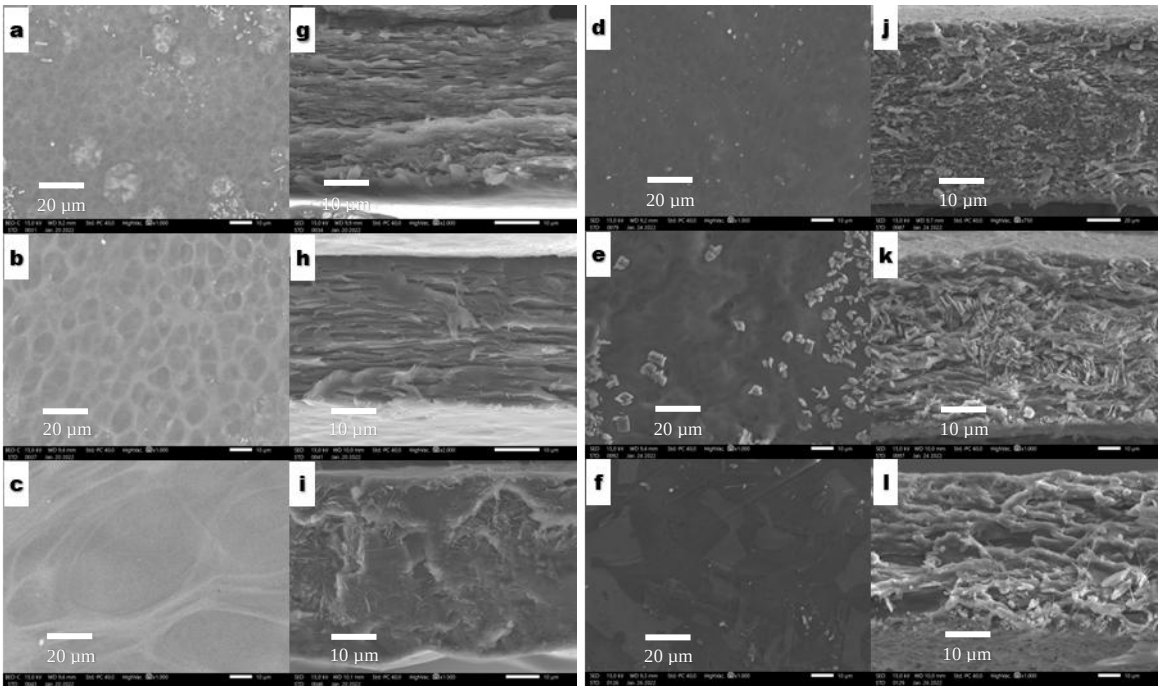


**Figure 2.** Surface morphology images of (a) KPL 10, (b) KPL25, (c) KPL50, (d) KPIL10, (e) KPIL25, and (f) KPIL40 at 1000×; Cross-section images of (g) KPL 10, (h) KPL25, (i) KPL50, (j) KPIL10, (k) KPIL25, and (l) KPIL40 at 2000×

### Atomic Content of Membrane Samples

The atomic contents of the six samples based on energy dispersive X-ray (EDX) spectra are displayed in Table 2. Boron atoms appeared in all spectra with a composition of 0% because the EDX method, in general, cannot detect elements with an atomic number lower than 11 (Boron atomic number is 5). Although a windowless EDX can detect elements with an atomic number from 5 upwards, occasionally, the results appear just like noise with a composition value of 0% [26]. Carbon atoms were detected in each sample because carbon is a main component of organic compounds, including chitosan, polyvinyl alcohol (PVA), acetic acid, and ionic liquid 1-hexyl-3-methylimidazolium iodide (HMII).

**Table 2.** Atomic contents of membrane samples

| Sample code | Content (%) | | | |
|---|---|---|---|---|
| | $C_6$ | $O_8$ | $Na_{11}$ | $I_{53}$ |
| KPL10 | 48.38 | 48.70 | 2.92 | 0 |
| KPL25 | 46.40 | 52.35 | 1.25 | 0 |
| KPL40 | 45.16 | 54.84 | 0 | 0 |
| KPIL10 | 49.53 | 38.35 | 0 | 12.02 |
| KPIL25 | 44.30 | 40.42 | 0 | 15.28 |
| KPIL40 | 18.76 | 54.91 | 23.34 | 2.99 |

The oxygen atom is also a main component of the materials used, such as chitosan, PVA, acetic acid, Lithium bis(oxalate) borate (LiBOB), and even ionic liquid HMII. The iodine atom was detected in all samples, but only three samples with ionic liquid HMII showed iodine atom content higher than zero. This was because the iodine atom was only present in one material, namely, the ionic liquid HMII. This result confirms that it succeeded in adding ionic liquid HMII into the membrane matrix of three samples.

Sodium atoms appeared in several samples through the chitosan preparation process (de-acetylation) using sodium hydroxide. In KPL samples, the content of sodium atoms decreased with the addition of LiBOB electrolytes because sodium ions have electronegativity similar to that of lithium ions. Thus, sodium ion may be used to stabilize $BOB^-$ ion. Meanwhile, in KPIL samples, sodium atoms only appeared in the KPIL40 sample. This may be caused by ionic liquid HMII, whose iodine ion can join with sodium ion to form sodium iodide, which was then dissolved in deionized water. The morphological structure of the KPIL40 sample was very uneven, as seen in Figure 2, so this may result in a large number of sodium atoms there.

### Fourier-transform Infrared Analysis (FTIR)

FTIR analysis examines the infrared spectra of the material tested. Each organic compound has at least one specific functional group, and each functional group has a specific transmittance trough when passed by an infrared ray. FTIR spectra analysis was conducted by comparing the spectra result with the database from [27]. The FTIR spectra of six samples are shown in Figure 3, and the functional group analysis is in Table. 3.

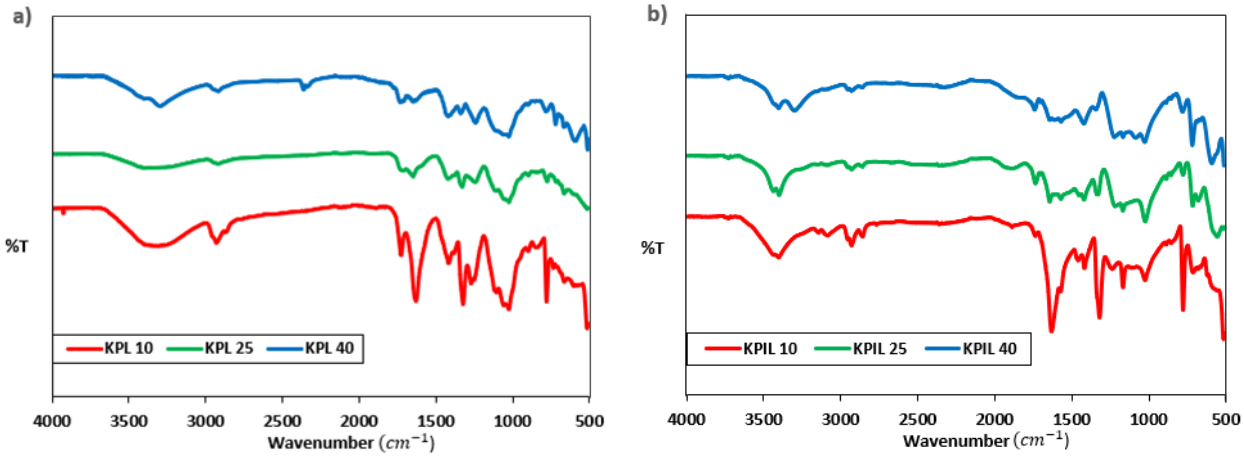


**Figure 3.** FTIR spectra of (a) KPL and (b) KPIL samples

There is no significant difference among the three variations of LiBOB electrolyte composition in both KPL and KPIL samples. The intensity of % transmittance changed slightly with the addition of LiBOB electrolyte. This

may indicate that the LiBOB electrolyte did not react with the composite membranes; it was mixed with the membrane. In KPL samples, there is a broad transmittance with an intermediate intensity above 3000 $cm^{-1}$, while in KPIL samples, there is a double transmittance with an intermediate intensity above 3000 $cm^{-1}$. Broad transmittance with intermediate intensity above 3000 $cm^{-1}$ is attributed to the hydroxyl group (–OH) of PVA and chitosan. Double transmittance with intermediate intensity above 3000 $cm^{-1}$ is attributed to the amine group (–NH) of chitosan and ionic liquid. Double vibration of the amine group appeared in KPIL samples as we added ionic liquid HMII, as seen from the chemical structure of ionic liquid HMII in Figure 4. The transmittance trough below 3000 $cm^{-1}$ (2700–2800 $cm^{-1}$) is attributed to the hydrocarbon group (–CH) of chitosan, PVA, acetic acid, and ionic liquid HMII. The trough at 1600–1800 $cm^{-1}$ is attributed to the primary amine group ($–NH_2$) of chitosan. The trough at 1400–1500 $cm^{-1}$ is attributed to the double bond carbon group (C=C) of PVA and ionic liquid HMII. The trough at 1300–1400 $cm^{-1}$ is attributed to the C–N group of chitosan and ionic liquid HMII. The trough at 1000–1100 $cm^{-1}$ is attributed to the secondary alcohol group of PVA and chitosan.

**Table 3.** FTIR transmittance troughs as a characteristic of the functional groups [27]

| Wavelength ($cm^{-1}$) | Intensity | Trough Type | Functional group |
|---|---|---|---|
| Above 3000 | Medium, High | Broad | O-H |
| Above 3000 | Medium, High | Double | N-H |
| 2700-2800 | Medium, High | Sharp | C-H |
| 1600-1800 | High | Sharp | $-NH_2$ |
| 1400-1500 | High | Sharp | -C=C |
| 1300-1400 | High | Sharp | C-N |
| 1000-1100 | Medium, High | Sharp | Secondary alcohol (-C-OH) |

The addition of ionic liquid HMII, which has an amine group, increased the concentration of amines so that the transmittance trough of KPIL membranes looks sharper and nearly like a double trough. That means amine groups were more dominant in KPIL, with assistance from the amine group of HMII shown in Figure 4.

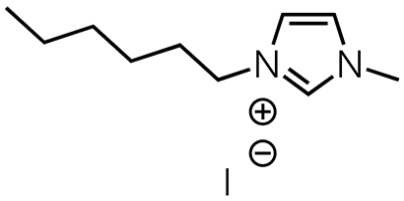


**Figure 4.** Chemical structure of ionic liquid HMII

### Stress and Strain Analysis

A solid polymer electrolyte (SPE) membrane needs to exhibit excellent mechanical strength, considering its application in folding and pulling repeatedly to fill up a particular space. Thus, analysis of maximum stress and maximum strain of the membrane is very important to ascertain its quality. Table 4 displays the maximum strain, tensile strength, and elastic modulus of each sample of SPE. There is no characteristic value of the KPL10 sample because it broke during handling even before the test started, indicating a very brittle characteristic of this sample. KPIL25 sample produced the highest maximum strain value, 1.14%, while KPIL40 produced the lowest maximum strain value, 0.3%. The membrane dimension affects its maximum strain: the larger the dimension, the higher the maximum strain. By possessing the highest thickness, the KPL40 sample produced the lowest maximum strain value, indicating that the mechanical strength of this sample greatly failed to meet the desired criteria.

On the tensile strength value, the KPIL25 sample produced the highest result (21.11 MPa), while the KPL40 sample produced the lowest result (2.20 MPa). A similar result was given by the previous study for the ionic liquid effect conducted by Ndruru et al. (2021), which used [EMIm]Ac ionic liquid for cellulose-based membranes; the optimum ionic liquid addition resulted in high mechanical strength with 20.83 MPa for tensile strength [28]. These results reflect the size effect: when the thickness of the membrane increases, its tensile strength and elastic modulus will decrease. However, based on general results, KPIL samples produced higher mechanical properties than KPL samples. This indicates that the addition of ionic liquid HMII to the membrane increased its mechanical properties. On the other hand, increasing the composition of LiBOB electrolyte to the membrane produced an

unspecified effect. There might be any other specific interaction between HMII ionic liquid and LiBOB electrolyte.

**Table 4.** Mechanical properties of membrane samples

| Sample Code | Thickness (mm) | Max Strain (%) | Tensile Strength (MPa) | Elastic Modulus (MPa) |
|---|---|---|---|---|
| KPL10 | - | - | - | - |
| KPL25 | 0.11 | 0.60 | 4.42 | 0.25 |
| KPL40 | 0.4 | 0.54 | 2.20 | 0.25 |
| KPIL10 | 0.06 | 1.08 | 13.01 | 1.10 |
| KPIL25 | 0.09 | 1.14 | 21.11 | 1.93 |
| KPIL40 | 0.17 | 0.30 | 3.76 | 1.12 |

### Electrochemical Impedance Spectroscopy (EIS) Analysis

To analyze the electrochemical properties of membrane samples, especially the interfacial area, electrochemical impedance spectroscopy is a simple and suitable technique. The impedance spectra from the EIS analysis result were fitted in the Nyquist plot and shown in Figure 5.

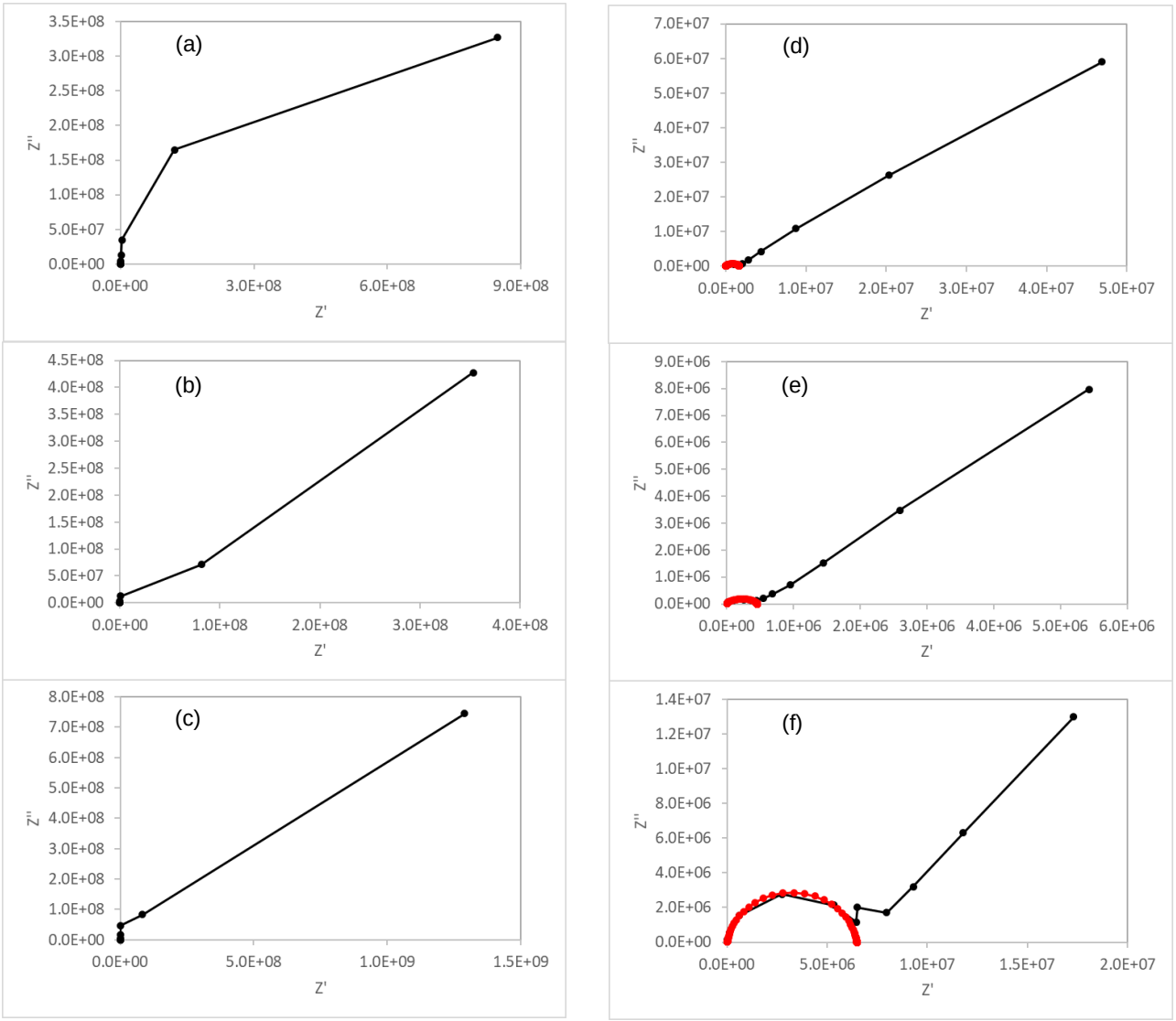


**Figure 5.** Impedance curve of (a) KPL10, (b) KPL25, (c) KPL40, (d) KPIL10, (e) KPIL25, and (f) KPIL40

From Figure 5, a semicircle pattern was found in the high-frequency region of all KPIL samples but not in KPL samples. The semicircle pattern appears as a parallel combination of both resistance and capacitance of the bulk electrolyte, which resulted from the migration process of proton ions and the immobilized state of polymer chains, respectively [29]. The absence of semicircle pattern in impedance analysis can be attributed to various

factors, including material homogeneity, frequency range selection, complexity of electrochemical processes, and measurement methodology [30]–[33]. The diameter of semicircles is the bulk resistance of the material, so the highest bulk resistance is in KPIL40, and the lowest is in KPIL25. Ionic conductivity can be calculated using Equation (1) to complete Table 5.

$$\sigma = \left(\frac{1}{Rb}\right) x \left(\frac{t}{A}\right) \quad (1)$$

Rb is the bulk resistance of the polymer electrolyte film, $\sigma$ is the ionic conductivity, t is the polymer electrolyte film thickness, and A is the film surface area.

**Table 5.** Electrical resistivity and ionic conductivity of KPIL membrane samples

| Item | Rb (Ω) | A ($cm^2$) | t (cm) | σ (S/cm) |
|---|---|---|---|---|
| KPIL10 | $1.96 \times 10^6$ | 2.8364 | 0.0172 | $3.10 \times 10^{-9}$ |
| KPIL25 | $5.57 \times 10^5$ | 2.8364 | 0.0115 | $7.28 \times 10^{-9}$ |
| KPIL40 | $6.85 \times 10^6$ | 2.8364 | 0.0271 | $1.40 \times 10^{-9}$ |

Table 5 shows the results of Equation (1). The highest ionic conductivity of KPIL samples is with 25% composition of LiBOB electrolyte, with $7.28 \times 10^{-9}$ S/cm. Increasing LiBOB electrolyte composition from 10% to 25% also increased the ionic conductivity of the membrane. In contrast, increasing it from 25% to 40% reduced the ionic conductivity of the membrane. Theoretically, adding more electrolytes to the membrane composition will improve ion mobility through the membrane so that the ionic conductivity of the membrane will be increased. The reduction of ionic conductivity from KPIL25 to KPIL40 may be influenced by ionic liquid viscosity, crystallinity, and ion aggregation, which were usually increased with adding LiBOB electrolyte composition [34]–[38]. No semicircle in KPL samples means that the ionic mobility occurred by diffusion mechanisms, or maybe the frequency range is not suitable [29]. However, this condition indicated that the bulk resistance of all KPL samples was higher than that of KPIL samples. Therefore, another type of ionic liquid needed to be tried to minimize viscosity, crystallinity, and ion aggregation potency in further studies. Making more variations of LiBOB electrolyte composition between 25% to 40% is also an option to determine the optimal composition of LiBOB electrolyte composition.

## CONCLUSION

No differences were identified between the three variations of Lithium bis(oxalate) borate (LiBOB) composition in Fourier-transform infrared (FTIR) transmittance troughs, which indicated that LiBOB concentration did not affect the functional group of membranes. There was a change in the FTIR spectra trough above 3000 $mm^{-1}$. A single trough for KPL samples and double troughs for KPIL samples indicated the addition of an amine group from ionic liquid 1-hexyl-3-methylimidazolium iodide (HMII) in KPIL samples. Scanning electron microscope (SEM) images show us that the addition of ionic liquid HMII decreased the compactness of membranes and improved the porosity of membranes. In this research, adding ionic liquid HMII significantly improved the mechanical strength of membranes, particularly tensile strength and modulus elasticity. The impedance plot of the KPL samples indicates a diffusion process, while the KPIL samples indicate an ionic migration process. The highest ionic conductivity is in KPIL25 with $7.28 \times 10^{-9}$ S/cm, and the lowest is in KPIL40 with $1.40 \times 10^{-9}$ S/cm.

## REFERENCES


[1] A. Saal, T. Hagemann, and U.S. Schubert. “Polymers for Battery Applications – Active Materials, Membranes, and Binders.” *Advanced Energy Materials*, vol. 11, no. 43, p. 2001984, 2020.

[2] J. Sheng, S. Tong, H. Zhibin, and R. Yang. “Recent Developments of Cellulose Materials for Lithium-ion Battery Separators.” *Springer Science & Business Media B*, Vol. 24, no. 1, pp. 4103–4122, 2017.

[3] R. Korthauer (Ed.). *Lithium-Ion Batteries: Basics and Applications*, Springer Berlin Heidelberg, 2018.

[4] A. Manthiram, X. Yu, and S. Wang. “Lithium Battery Chemistries Enabled by Solid-State Electrolytes.” *Nature Reviews Materials*, vol. 2, p. 16103, 2017.

[5] X. Wu, K. Pan, M. Jia, Y. Ren, H. He, L. Zhang, and S. Zhang. “Electrolyte for Lithium Protection: from Liquid to Solid.” *Green Energy and Environment*, vol. 4, no. 4, pp. 360–374, 2019.

[6] M. Kotobuki. *Polymer Electrolytes*. Wiley Online Library, 2019.

[7] M.H. Rahman, M. Sofiuzzaman, M.I.H. Mondal, A. Rahman, F. Ahmed, M.M. Islam, and M.A. Habib. "Recent Advancement of PVA/Chitosan-Based Composite Biofilm for Food Packaging." *Biomedical Journal of Science & Technological Research*, vol. 46, no. 1, pp. 36982–36986, 2022.

[8] N.A. Rahman, S.A Hanifah, N.N. Mobarak, A. Ahmad, N.A. Ludin, F. Bella, and M.S. Su'ait. "Chitosan as a Paradigm for Biopolymer Electrolytes in Solid-state-dye-sensitised Solar Cells." *Polymer*, vol. 230, p. 124092, 2021.

[9] R.A.O. Bernal, R.O. Olekhnovich, and M.V. Uspenskaya. "Chitosan/PVA Nanofibers as Potential Material for the Development of Soft Actuators." *Polymers*, vol. 15, no. 9, 2023.

[10] D.F. Zatalini, E. Hendradi, P. Drake, and R. Sari. "The Effect of Chitosan and Polyvinyl Alcohol Combination on Physical Characteristics and Mechanical Properties of Chitosan-PVA-Aloe vera Film." *Jurnal Farmasi dan Ilmu Kefarmasian Indonesia*, vol. 10, no. 2, pp. 151–161, 2023.

[11] I. Saini, A. Sharma, R. Dhiman, S. Aggarwal, S. Ram, and P.K. Sharma. "Grafted SiC Nanocrystal: For Enhanced Optical, Electrical, and Mechanical Properties of Polyvinyl Alcohol." *Journal of Alloy Compound*, vol. 714, pp. 172–180, 2017.

[12] J.O. Dennis, M.F. Shukur, O.A. Aldaghri, K.H. Ibnaouf, A.A. Adam, F. Usman, Y.M. Hassan, A. Alsadig, W.L. Danbature, and B.A. Abdulkadir. "A Review of Current Trends on Polyvinyl Alcohol (PVA)-Based Solid Polymer Electrolytes." *Molecules*, vol. 28, no. 4, 2023.

[13] S. Cavus and E. Durgun. "Poly(vinyl alcohol)-Based Polymer Gel Electrolytes: Investigation on Their Conductivity and Characterization." *Acta Physica Polonica A*,vol. 129, no. 4, pp. 621–624, 2016.

[14] E.Y. Wardhono, M.P. Pinem, S. Susilo, B,J, Siom, A. Sudrajad, A. Pramono, Y. Meliana, and E. Guénin. "Modification of Physio-Mechanical Properties of Chitosan-Based Films via Physical Treatment Approach." *Polymers*, vol. 14, no. 23, p. 5216, 2022.

[15] R.K. Cheedarala and J.I. Song. "Moderately Transparent Chitosan-PVA Blended Membrane for Strong Mechanical Stiffness and as a Robust Bio-Material Energy Harvester through Contact-Separation Mode TENG." *Front. Nanotechnology*, vol. 3, p. 667453, 2021.

[16] D. Permana, E. Ilimu, N.M. Faariu, A. Setyawati, L.O. Kadidae, and L.O.A.N Ramadhan. "Synthesis and Characterization of Chitosan-Polyvinyl Alcohol-$Fe_2O_3$ Composite Membrane for DMFC Application." *Makara Journal of Science*, vol. 24, no. 1, pp. 1–9, 2020.

[17] A. Benouar and M.R.A. Bacha. "Ionic Conductivity of Chitosan-Lithium Electrolyte in Biodegradable Battery Cell." *Indonesian Journal of Chemistry*, vol. 20, no. 3, pp. 655–660, 2020.

[18] E.M. Wigayati, T. Lestariningsih, C.R. Ratri, I. Purawiardi, and B. Prihandoko. "Synthesis of LiBOB Fine Powder to Increase Solubility." *Makara Journal of Technology*, vol. 21, no. 1, pp. 26–32, 2017.

[19] N.M. Khan, N.F. Mazuki, and A.S. Samsudin. "Contribution of $Li^+$ Ions to a Gel Polymer Electrolyte Based on Polymethyl Methacrylate and Polylactic Acid Doped with Lithium Bis(oxalato) Borate." *Journal of Electronic Materials*, vol. 51, pp. 745–760, 2022.

[20] Y. Yuan, X. Peng, B. Wang, K. Xue, Z. Li, Y. Ma, B. Zheng, Y. Song, and H. Lu. "Solvate ionic liquid-derived solid polymer electrolyte with lithium bis(oxalato) borate as a functional additive for solid-state lithium metal batteries." *Journal of Materials Chemistry A*, vol. 11, no. 3, pp. 1301–1311, 2023.

[21] M. Gamba, A.A.M. Lapis, and J. Dupont. "Supported Ionic Liquid Enzymatic Catalysis for the Production of Biodiesel." *Advanced Synthesis and Catalysis*, vol. 350, no. 1, pp. 160–164, 2008.

[22] E. Ghasemian, M. Najafi, A.A. Rafati, and Z. Felegari. "Effect of Electrolytes on Surface Tension and Surface Adsorption of 1-hexyl-3-methylimidazolium chloride Ionic Liquid in Aqueous Solution." *Journal of Chemistry and Thermodynamics*, vol. 42, no. 8, pp. 962–966, 2010.

[23] M.H. Khanmirzaei. S.Ramesh, and K.Ramesh. "Effect of 1-Hexyl-3-Methylimidazolium Iodide Ionic Liquid on Ionic Conductivity and Energy Conversion Efficiency of Solid Polymer Electrolyte-Based Nano-Crystalline Dye-Sensitized Solar Cells." *Journal of Nanoscience and Nanotechnology*, vol. 20, no. 4, pp. 2423–2429, 2020.

[24] J.W. Chew, M.H. Khanmirzaei, A. Numan, F.S. Omar, K. Ramesh, and S. Ramesh. "Performance studies of ZnO and multi walled carbon nanotubes-based counter electrodes with gel polymer electrolyte for dye-sensitized solar cell." *Materials Science in Semiconductor Processing*, vol. 83, pp. 144–149, 2018.

[25] D. Qin, Y. Zhang, S. Huang, Y. Luo, D. Li, and Q. Meng. “Ionic liquid/polymer composite electrolytes by in situ photopolymerization and their application in dye-sensitized solar cells.” *Electrochimica Acta*, vol. 56, no. 24, pp. 8680–8687, 2011.

[26] J.S. Heslop-Harisson. “Energy Dispersive X-Ray Analysis,” in *Physical Methods in Plant Sciences*, H.-F. Linskens and J.F. Jackson, Eds. Berlin, Heidelberg: Springer Berlin Heidelberg, 1990, pp. 144–277.

[27] R.M. Silverstein, F.X. Webster, and D. Kiemle. *Spectrometric Identification of Organic Compounds Handbook*, 7th ed., Wiley Interscience, 2005.

[28] S.T.C.L. Ndruru, E. Pramono, D. Wahyuningrum, B. Bundjali, and I.M. Arcana. “Preparation and characterization of biopolymer blend electrolyte membranes based on derived celluloses for lithium-ion batteries separator.” *Bulletin of Materials Science*, vol. 44, no. 104, 2021.

[29] S.B. Aziz, M.H. Hamsan, M.M. Nofal, W.O. Karim, I. Brevik, M.A. Brza, R.T. Abdulwahid, S. Al-Zangana, and M.F.Z. Kadir. “Structural, Impedance and Electrochemical Characteristics of Electrical Double Layer Capacitor Devices Based on Chitosan: Dextran Biopolymer Blend Electrolytes.” *Polymers-MDPI*, vol. 12, no. 6, 2020.

[30] V.A. Skryshevsky, Y.S. Milovanov, I.V. Gavrilchenko, S.I. Tiagulskyi, A.V. Rusavsky, V.S. Lysenkoet, and A.N.Nazarov. "Impedance spectroscopy of single graphene layer at gas adsorption." *Physica Status Solidi (A)*, vol. 212, no. 9, p. 1941–1945, 2015.

[31] E.L. Anderson and P. Bühlmann. "Electrochemical impedance spectroscopy of ion-selective membranes: artifacts in two-, three-, and four-electrode measurements." *Analytical Chemistry*, vol. 88, no. 19, pp. 9738–9745, 2016.

[32] B.B. Zhang, G. H. Wu, C.B. Chen, and S. Gao. "Solid propellant aging detection method based on impedance spectroscopy." *Advanced Materials Research*, vol. 1179, p. 133–144, 2024.

[33] X. Wang, H. Zhao, A. Wang, Z. Dong, Y. Fan, and Z. Zhai. "A portable impedance spectroscopy measurement method through adaptive reference resistance." *IEEE Access*, vol. 9, pp. 88011-88018, 2021.

[34] S. Gupta, P. Singh, and B. Bhattacharya. "Change in charge carrier dynamics by incorporating ionic liquid into poly ethylene oxide–based sodium acetate polymer electrolytes." *High Performance Polymers*, vol. 34, no. 6, p. 683– 690, 2022.

[35] S.K. Chaurasia, A.L Saroj, Shalu, V.K. Singh, A.K. Tripathi, A.K Gupta, Y.L. Verma, and R.K. Singh. "Studies on structural, thermal and AC conductivity scaling of PEO-LI$PF_6$ polymer electrolyte with added ionic liquid [BMIM$PF_6$]." *AIP Advances*, vol. 5, p. 077178, 2015.

[36] K. Nakabayashi, Y. Sato, Y. Isawa, C. Lo, and H. Mori. "Ionic conductivity and assembled structures of imidazolium salt-based block copolymers with thermoresponsive segments." *Polymers*, vol. 9, no. 11, p. 616, 2017.

[37] E. Coletta, M.F. Toney, and C.W. Frank. "Influences of liquid electrolyte and polyimide identity on the structure and conductivity of polyimide–poly(ethylene glycol) materials." *Journal of Applied Polymer Science*, vol. 132, no. 12, 2014.

[38] A.R. Polu, P.K. Singh, P.S. kumar, G.M. Joshi, T. Ramesh, I.M. Noor, A.Y. Madkhli, and S. Kakroo. "Development of solid polymer electrolytes based on poly (ethylene oxide) complexed with 2-trifluoromethyl-4, 5-dicyanoimidazole lithium salt and 1-ethyl-3-methylimidazolium bis(trifluoromethylsulfonyl)imide ionic liquid for Li-ion batteries." *High Performance Polymers*, vol. 35, no. 1, pp. 4–9, 2022.